

Table 2. Alice-measured emission line brightness averages and SDs in sunlight and eclipse.

Emission line	Type	Disk-average brightness (rayleighs)		
		IEclipse01	IEclipse04	IEclipse05
OI 130.4 nm	Sunlight	706 ± 134	445 ± 27	347 ± 142
	Eclipse	597 ± 43	394 ± 14	254 ± 71
	Ratio S/E	1.18 ± 0.24	1.12 ± 0.08	1.37 ± 0.68
OI 135.6 nm	Sunlight	882 ± 177	577 ± 35	480 ± 188
	Eclipse	797 ± 57	536 ± 18	381 ± 94
	Ratio S/E	1.11 ± 0.24	1.08 ± 0.08	1.26 ± 0.58
SI 147.9 nm	Sunlight	1167 ± 271	986 ± 54	596 ± 288
	Eclipse	1205 ± 87	874 ± 28	429 ± 144
	Ratio S/E	0.97 ± 0.24	1.13 ± 0.07	1.39 ± 0.82

NH Long Range Reconnaissance Imager (LORRI) images (17). This same feature appears in the HST/SBC image in Fig. 2B, obtained when East Giru was shifted just behind the limb. The auroral feature near East Giru in both LORRI and HST/SBC images is ~15° northward of Jupiter's field line tangent point at the limb, which suggests that ionospheric currents are diverted northward from this nominal position toward a region of higher gas density near the plume. Similar deviations of the anti-jovian FUV emissions from nominal tangent points observed with STIS are likely caused by the prevalence and distribution of plumes there (21). Volcanic plume aurorae were not identified in previous lower-quality STIS FUV images, which caused an apparent discrepancy with visible images of plume aurorae. The East Giru plume FUV auroral feature in Fig. 2 resolves this discrepancy and reveals the influence of plumes on Io's electrodynamic interaction. The upstream-side emission feature is more apparent when limb brightened at viewing geometries like those reported in Fig. 2. This feature was predicted by aurora image simulations (22) and is diagnostic of the divergence of the plasma flow upstream of Io, a primary trait of Io's interaction with the plasma torus.

References and Notes

1. F. Bagenal, *J. Atmos. Sol. Terres. Phys.* **69**, 387 (2007).
2. E. Lellouch, M. A. McGrath, K. L. Jessup, in *Io After Galileo* (Springer-Praxis, UK, 2006), pp. 231–264.
3. J. Pearl *et al.*, *Nature* **280**, 755 (1979).
4. W. M. Sinton, C. Kaminski, *Icarus* **75**, 207 (1988).
5. J. R. Spencer *et al.*, *Science* **288**, 1198 (2000).
6. A. F. Cook *et al.*, *Science* **211**, 1419 (1981).
7. J. T. Clarke, J. Ajello, J. Luhmann, N. M. Schneider, I. Kanik, *J. Geophys. Res.* **99**, 8387 (1994).
8. P. E. Geissler *et al.*, *Science* **285**, 870 (1999).
9. A. H. Bouchez, M. E. Brown, N. M. Schneider, *Icarus* **148**, 316 (2000).
10. P. E. Geissler *et al.*, *J. Geophys. Res.* **106**, 26137 (2001).
11. P. E. Geissler *et al.*, *Icarus* **172**, 127 (2004).
12. I. DePater *et al.*, *Icarus* **156**, 296 (2002).
13. K. D. Retherford, thesis, The Johns Hopkins University (2002).
14. J. Saur, D. F. Strobel, *Icarus* **171**, 411 (2004).
15. S. A. Stern *et al.*, in *Astrobiology and Planetary Missions*, R. B. Hoover, G. V. Levin, A. Y. Rozanov, G. R. Gladstone, Eds. (Proc. SPIE, Volume 5906, 2005), pp. 358–367.
16. K. D. Retherford *et al.*, paper presented at the Magnetospheres of the Outer Planets Meeting, San Antonio, TX, 25 June, 2007.
17. J. R. Spencer *et al.*, *Science* **318**, 240 (2007).
18. The angular size of Io varies with spacecraft distance but is smaller than the Alice slit width for these data. The spectral resolution varies between 0.3 nm and ~0.9 nm

for emissions known to be located near the satellite disk (22); see, e.g., Fig. 2.

19. H. C. Ford *et al.*, in *Future EUV/UV and Visible Space Astrophysics Missions and Instrumentation*, J. C. Blades, O. H. W. Siegmund, Eds. (Proc. SPIE, Volume 4854, 2003), pp. 81–94.
20. F. L. Roesler *et al.*, *Science* **283**, 353 (1999).
21. K. D. Retherford *et al.*, *J. Geophys. Res.* **105**, 27157 (2000).

22. J. Saur, F. M. Neubauer, D. F. Strobel, M. E. Summers, *Geophys. Res. Lett.* **27**, 2893 (2000).
23. K. D. Retherford, H. W. Moos, D. F. Strobel, *J. Geophys. Res.* **108**, 1333 (2003).
24. L. M. Feaga, thesis, The Johns Hopkins University (2005).
25. K. L. Jessup *et al.*, *Icarus* **169**, 197 (2004).
26. J. R. Spencer *et al.*, *Icarus* **176**, 283 (2005).
27. P. D. Feldman *et al.*, *Geophys. Res. Lett.* **27**, 1787 (2000).
28. D. F. Strobel, B. C. Wolven, *Astrophys. Space Sci.* **277**, 271 (2001).
29. F. Neubauer, *J. Geophys. Res.* **103**, 19843 (1998).
30. F. M. Neubauer, *J. Geophys. Res.* **104**, 3863 (1999).
31. We thank the New Horizons mission and science teams. New Horizons is funded by NASA. Support for this work was also provided by NASA through grant number GO-10871 from the Space Telescope Science Institute (STScI), which is operated by the Association of Universities for Research in Astronomy, Inc., under NASA contract NAS5-26555.

Supporting Online Material

www.sciencemag.org/cgi/content/full/318/5848/237/DC1
Figs. S1 and S2
Tables S1 and S2

10 July 2007; accepted 19 September 2007
10.1126/science.1147594

REPORT

Io Volcanism Seen by New Horizons: A Major Eruption of the Tvashtar Volcano

J. R. Spencer,^{1*} S. A. Stern,² A. F. Cheng,² H. A. Weaver,³ D. C. Reuter,⁴ K. Retherford,⁵ A. Lunsford,⁴ J. M. Moore,⁶ O. Abramov,¹ R. M. C. Lopes,⁷ J. E. Perry,⁸ L. Kamp,⁷ M. Showalter,⁹ K. L. Jessup,¹ F. Marchis,⁹ P. M. Schenk,¹⁰ C. Dumas¹¹

Jupiter's moon Io is known to host active volcanoes. In February and March 2007, the New Horizons spacecraft obtained a global snapshot of Io's volcanism. A 350-kilometer-high volcanic plume was seen to emanate from the Tvashtar volcano (62°N, 122°W), and its motion was observed. The plume's morphology and dynamics support nonballistic models of large Io plumes and also suggest that most visible plume particles condensed within the plume rather than being ejected from the source. In images taken in Jupiter eclipse, nonthermal visible-wavelength emission was seen from individual volcanoes near Io's sub-Jupiter and anti-Jupiter points. Near-infrared emission from the brightest volcanoes indicates minimum magma temperatures in the 1150- to 1335-kelvin range, consistent with basaltic composition.

The New Horizons (NH) Jupiter flyby provided the first close-up observations of the tidally driven volcanism of Jupiter's moon Io since the last Galileo orbiter observations of Io in late 2001 (1). The closest approach to Io occurred at 21:57 UT on 28 February 2007 at a range of 2.24 million km. Sunlit observations were made at solar phase angles from 5° to 159°, and four eclipses of Io by Jupiter were also observed. NH obtained 190 Io images with its 4.96 μrad per pixel panchromatic (400 to 900 nm) Long-Range Reconnaissance Imager (LORRI) and 17 color nighttime and eclipse images with the 20 μrad per pixel Multicolor Visible Imaging Camera (MVIC), although MVIC coverage of Io's day side was not possible because of detector saturation. NH also obtained seven 1.25- to 2.5-μm near-infrared image cubes at 62 μrad per pixel with the Linear Etalon Infrared Spectral Array instrument

(LEISA) and numerous disk-integrated ultraviolet observations with the Alice instrument, discussed separately (2).

Eleven volcanic plumes were identified in the NH images (Fig. 1A and table S1). In addition to the single very large "Pele-type" plume at Tvashtar, which is described separately, NH observed 10 SO₂-rich "Prometheus-type" plumes (3–5). These smaller plumes averaged 80 km high and varied greatly in brightness. Plumes seen for the first time by NH include those at Zal and Kurdalagon and a large new plume, 150 km high, at north Lema Regio, which has produced a large albedo change. Three of these plumes, north Lema and north and south Masubi, are associated with recent large lava flows, supporting the idea that Prometheus-type plumes result from mobilization of surface volatiles by active lava flows. All active plumes that were on

the disk or near the limb were also visible in Jupiter eclipse images because of excitation of plume gases by the jovian magnetosphere (Fig. 2B), as also seen by Galileo (6).

¹Southwest Research Institute, 1050 Walnut Street, Suite 300, Boulder, CO 80302, USA. ²NASA Headquarters, Washington, DC 20546, USA. ³Applied Physics Laboratory, Johns Hopkins University, 11100 Johns Hopkins Road, Laurel, MD 20723, USA. ⁴NASA Goddard Space Flight Center, Greenbelt, MD 20771, USA. ⁵Southwest Research Institute, Post Office Drawer 28510, San Antonio, TX 78228, USA. ⁶NASA Ames Research Center, Moffett Field, CA 94035, USA. ⁷Jet Propulsion Laboratory, 4800 Oak Grove Drive, Pasadena, CA 91109, USA. ⁸Lunar and Planetary Laboratory, University of Arizona, Tucson, AZ 85721, USA. ⁹Search for Extraterrestrial Intelligence (SETI) Institute, 515 North Whisman Road, Mountain View, CA 94043, USA. ¹⁰Lunar and Planetary Institute, 3600 Bay Area Boulevard, Houston, TX 77058, USA. ¹¹European Southern Observatory, Casilla 19001, Santiago 19, Chile.

*To whom correspondence should be addressed. E-mail: spencer@boulder.swri.edu

LORRI imaged almost all of Io at relatively low phase angles with resolutions between 14 and 22 km per pixel, providing a surface albedo map suitable for comparison with previous maps (7) (Fig. 1A). There are at least 19 locations where surface changes have occurred since Galileo's last global images, taken between 1999 and 2001 (Fig. 1A). The number of surface changes detected is only one-fourth of those detected during the 5-year Galileo mission (8), perhaps because of NH's lower spatial resolution, the lack of a color data set with comparable resolution, and the possibility of surface changes that have faded since their formation.

The large plume at Tvashtar has renewed the large ring-shaped plume deposit seen at Tvashtar in 2000 (1), which had been obscured by other plume deposits by mid-2001. A two-lobed plume deposit surrounds a new, 240-km-long dark feature, probably a lava flow, at Masubi (Fig. 1, B to D) created

by the two plumes observed by NH: "North Masubi" near the vent and "South Masubi" at the distal flow front. This flow is the longest new lava flow to be erupted on Io since the 1979 Voyager images. The North Lema volcanic plume has produced a 700-km-wide concentric deposit (Fig. 1, E and F) surrounding a fresh, 130-km-long apparent dark lava flow. Other late-Galileo-era plume deposits, notably around Dazhbog and Thor (8), have faded to invisibility.

LEISA observed 1.25- to 2.5- μm volcanic thermal emission from Io's night side or in Jupiter eclipse at almost all longitudes at a spatial resolution of 140 to 170 km per pixel, producing a uniform global snapshot of Io's high-temperature volcanic thermal emission (Fig. 1A). Thermal emission from several volcanoes was also seen in 0.4- to 1.0- μm LORRI images in Jupiter eclipse or on the night side (Fig. 2A). At least 36 hot spots were detected. All correspond to previously known active volcanic centers

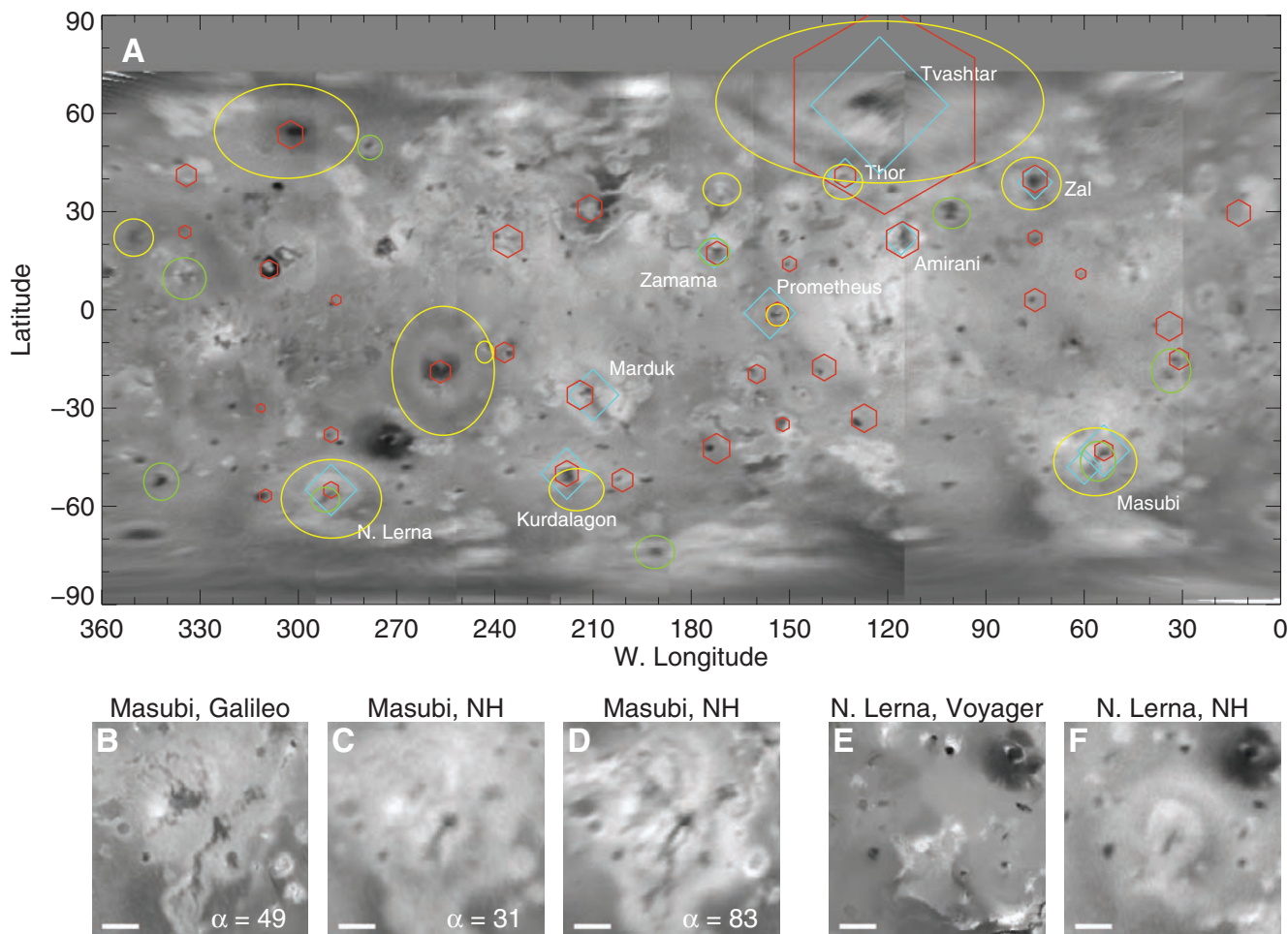


Fig. 1. (A) Global map of Io derived from eight LORRI images obtained at phase angles between 26° and 47°, showing volcanic activity detected by NH. See fig. S1 for an unannotated version. Yellow ovals denote areas with new, faded, or shifted plume or other volatile deposits since the last Galileo images in 2001. Green circles denote areas where probable new lava flows have occurred. Cyan diamonds indicate locations of active plumes (table S1), and orange hexagons are volcanic hot spots detected by LEISA. For plumes and hot spots, symbol size indicates the approximate relative size and brightness of the features. (B to F) Comparison of NH LORRI and earlier images (7) of major

surface changes at Masubi (45°S, 57°W) and North Lerna (55°S, 290°W), reprojected to a consistent geometry. The scale bars are 200 km long, and α is the solar phase angle. At Masubi, old lava flows seen by Voyager and Galileo (B) have been obscured at low phase angles (C) by plume deposits associated with what is probably a new dark lava flow. The old flows are still seen by NH at high phase angles (D), suggesting the plume deposits are not thick enough to obscure the surface texture of the old flows. At North Lerna, a recent eruption has generated a 130-km-long dark feature (F), probably a lava flow, as well as an active plume that has produced a concentric pattern of deposits.

New Horizons at Jupiter

(9) except for a bright new hot spot that we call “East Giru” at 22°N, 235°W, 130 km east of the known volcano Giru. This hot spot location corresponds to an inconspicuous dark linear feature, possibly an old fissure eruption, in Galileo images. No associated albedo change is visible in sunlit LORRI images; perhaps East Giru is a very young eruption that has not had time to produce observable albedo changes. No plume was seen in reflected light at East Giru, but a detached glow 330 km directly above the hot spot was seen in eclipse images (Fig. 2A), suggesting some associated gas output.

LORRI eclipse images show numerous faint point sources of emission (Fig. 2A), particularly near the sub-jovian and anti-jovian points (on the equator at longitudes 0° and 180°W), with a typical brightness of ~100 kRayleigh assuming a 15-km-by-15-km source region. These were also seen in Galileo eclipse images (6). These spots all correspond to low-albedo volcanic centers (Fig. 2D), but because simultaneous LEISA images show no corresponding cluster of bright spots in the near-infrared (Fig. 2, E and F), where volcanic thermal emission dominates, it is likely that a non-thermal mechanism, probably plasma-related, creates

the sub-jovian and anti-jovian clusters of point-source emission. Most of these spots are less than about 30 km in size, suggesting a near-surface origin.

A fortuitous major eruption of the Tvashtar volcano during the NH flyby provides a comprehensive view of a large, sulfur-rich Pele-class (3) volcanic plume on Io. Tvashtar, a series of calderas centered near 62°N, 122°W, has been one of Io’s most active volcanos in recent years. An active period from late 1999 to early 2001 (10–12) produced a large infrared hot spot, plume, and orange pyroclastic deposits and was followed by quiescent conditions seen in late 2001 (1, 13) and early 2003 and 2004. Renewed thermal emission in April to May 2006 (14) may have been an earlier phase of the 2007 eruption seen by NH. Continued thermal emission from Tvashtar was seen by ground-based observations during and after the NH encounter from 18 January (15) to 27 May 2007.

The 2007 Tvashtar plume was first seen in back-scattered light in 260-nm wavelength images from the Hubble Space Telescope (HST) on 14 February 2007 (Fig. 3A) and again in absorption in Jupiter transit images on 21 February (Fig. 3B). Absorption in the 260-nm wavelength region suggests, by analogy with previous HST observations of the Pele plume, that the Tvashtar plume is rich in S₂ gas (16), as also inferred from the orange color of its plume deposits seen previously by Galileo (12, 17).

NH imaged the Tvashtar plume on 39 occasions over 7.8 days, at phase angles between 7° and 159° and LORRI resolutions between 12 and 38 km per pixel. The plume height was remarkably constant, varying between roughly 320 and 360 km, and full width was about 1100 km, consistent with the diameter of the pyroclastic deposits (Fig. 1). The plume had a bright top in all images (Fig. 3, C, D, and F to J), very similar to Voyager images of the Pele plume: This morphology is not consistent with simple ballistic models of plume particle flight, as noted for Pele (18), but is consistent with hydrodynamic models with entrained particles that include a gas shock front at the top of the plume (19). Most Tvashtar plume images show little evidence for a central upgoing column of particles (e.g., Fig. 3C), suggesting that the observed particles may condense out of the plume rather than being directly ejected from the vent.

The plume contains remarkable time-variable filamentary structures similar to those glimpsed in the single high-resolution Voyager 1 image of the Pele plume. This structure allows tracing of motion within the plume in a sequence of five images of the upper part of the plume obtained at 2-min intervals on 1 March (Fig. 3, F to J, and movie S1). Speeds projected on the plane of the sky are 0.4 to 0.7 km s⁻¹ (Fig. 3E), comparable to expected ballistic ejection speeds for a 350-km-high plume (~1.0 km s⁻¹), and accelerate as plume features fall toward the surface. Features appear to slide down the upper surface of the plume rather than tracing ballistic trajectories originating at the vent.

The source of the Tvashtar plume is associated with by far the brightest hot spot seen by NH (Fig. 4).

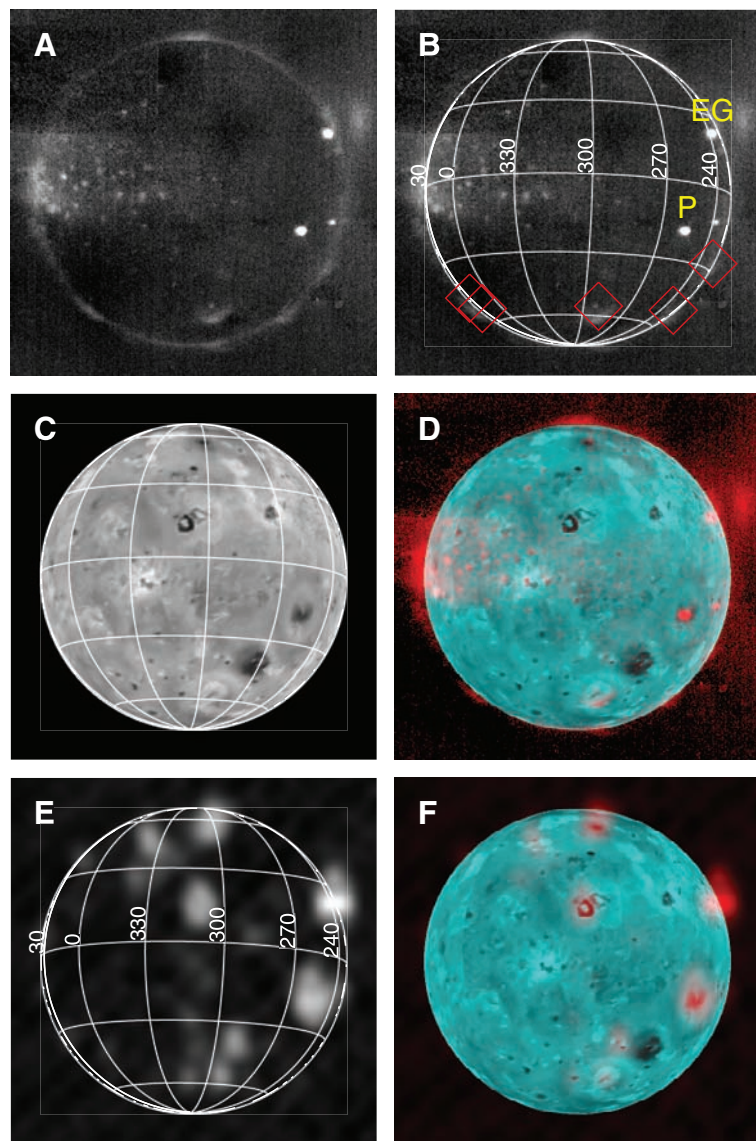
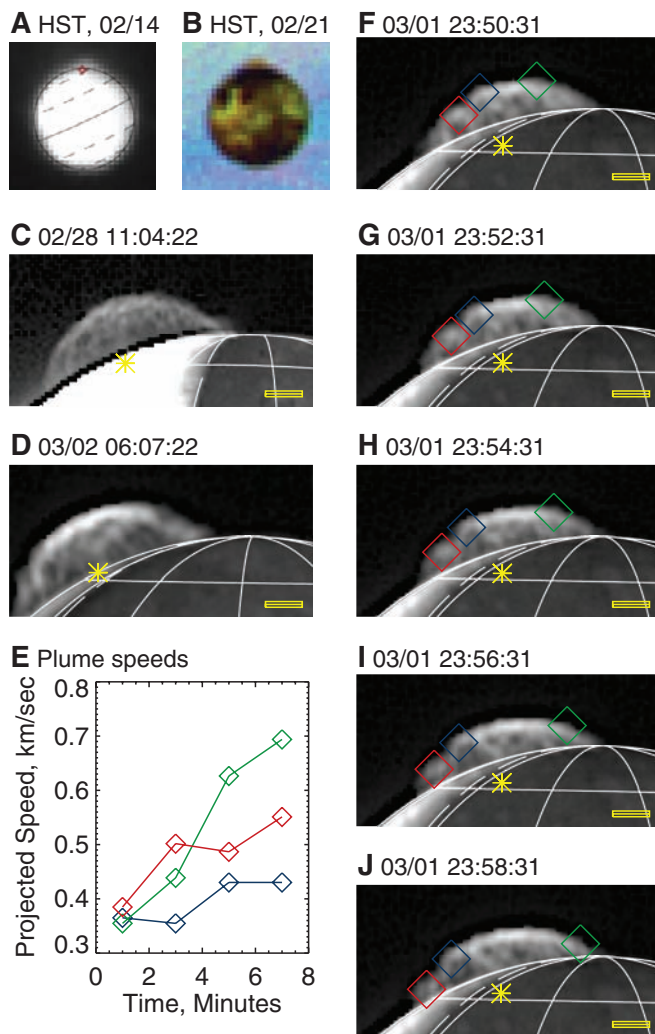


Fig. 2. Images of Io in Jupiter eclipse. (A) LORRI image taken at 27 February 14:37 UT with an effective exposure time of 16 s. Dark blotches and straight lines are artifacts. The brightest spots (P, Pele; EG, East Giru) are thermal emission from active volcanoes, and more diffuse emission is from the plumes and atmosphere (6). (B) Same image with latitude/longitude grid showing glowing plumes (plume sources, table S1, indicated by red diamonds). (C) Simulated sunlit view with the same geometry, based on sunlit LORRI images (Fig. 1A). (D) Combined sunlit (cyan) and eclipse (red) image, showing that all pointlike sources of emission in the eclipse image correspond to low-albedo volcanic centers. (E) A ~2.3- μ m LEISA eclipse image at 27 February 15:31 UT, showing thermal emission from active volcanoes. Elongation of the hot spots is an artifact. (F) Combined visible albedo (cyan) and LEISA thermal emission (red) image, showing the sources of the volcanic emission.

Fig. 3. The Tvashtar plume. **(A)** Discovery image by HST in backscattered light in the F255W filter (central wavelength = 260 nm). The red diamond indicates the plume source. **(B)** HST image of 260 nm absorption by the plume against Jupiter: 260 nm (blue) plus 330 nm (green) plus 410 nm (red) color composite. Other images are in visible light from NH LORRI. The scale bar is 200 km long, and the yellow star indicates the projected location of the hot spot at the plume source. The dashed line is the terminator. **(C)** Highest-resolution view of the full plume, at a resolution of 12.4 km per pixel and phase angle of 102°, showing the filamentary structure. Images are sharpened by unsharp masking; the dark line at the edge of the disk is an artifact of the sharpening. **(D)** Image at 145° phase angle at 22.4 km per pixel, showing the time variability of the details of the plume structure and the persistent bright top. **(F to J)** Sequence of frames at 2-min intervals showing dynamic in the upper part of the plume (the source is on the far side of Io). Colored diamonds track individual features whose speeds, projected on the plane of the sky, are shown in **(E)**.



Thermal emission was observed on multiple occasions by LORRI, LEISA, and by MVIC at wavelengths from 2.5 to below 0.7 μm . The hot spot location, 62.5°N, 122.5°W, coincides with the fire fountains seen at Tvashtar by Galileo in November 1999. The spectrum can be fit with a single temperature blackbody at 1287 K from 1.25 to 2.04 μm , providing a lower limit to the magma temperature, comparable to Galileo estimates (12). Assuming a temperature of 1200 K for the Tvashtar hotspot, an area of 49 km^2 is derived from the brightness in LORRI images, comparable to the $\sim 25 \text{ km}^2$ area of the incandescent fire fountain seen by Galileo at Tvashtar in November 1999 (12). The isothermal blackbody emission spectrum at close to magmatic temperatures is also consistent with an energetic eruption such as a fire fountain, rather than, for instance, spreading and cooling lava flows (20, 21). Temperatures are consistent with basaltic lava composition: Exotic high temperature magmas, inferred from some Galileo observations (22), are not required either at Tvashtar or other hot spots seen by NH.

References and Notes

1. E. P. Turtle *et al.*, *Icarus* **169**, 3 (2004).
2. K. D. Retherford *et al.*, *Science* **318**, 237 (2007).
3. A. S. McEwen, L. Soderblom, *Icarus* **55**, 191 (1983).
4. P. Geissler, D. Goldstein, in *Io After Galileo*, R. M. C. Lopes, J. R. Spencer, Eds. (Praxis, Chichester, UK, 2007), pp. 163–192.
5. “Pele-type” plumes are thought to result from direct ejection of gas from a volcanic vent, whereas the smaller “Prometheus-type” plumes may result from remobilization of surface volatiles by lava flows.
6. P. E. Geissler *et al.*, *J. Geophys. Res.* **106**, 26137 (2001).
7. U.S. Geological Survey Astrogeology Research Program, <http://astrogeology.usgs.gov/Projects/JupiterSatellites/fo.html>.
8. P. E. Geissler *et al.*, *Icarus* **172**, 127 (2004).
9. R. M. C. Lopes, J. Radebaugh, M. Meiner, J. Perry, F. Marchis, in *Io After Galileo*, R. M. C. Lopes, J. R. Spencer, Eds. (Praxis, Chichester, UK, 2007), pp. 307–323.
10. R. R. Howell *et al.*, *J. Geophys. Res.* **106**, 33129 (2001).
11. F. Marchis *et al.*, *Icarus* **160**, 124 (2002).
12. M. P. Milazzo *et al.*, *Icarus* **179**, 235 (2005).
13. F. Marchis *et al.*, *Icarus* **176**, 96 (2005).
14. C. Laver, I. de Pater, F. Marchis, *Bull. Am. Astron. Soc.* **38**, 612 (2006).
15. J. A. Rathbun, J. R. Spencer, paper presented at the 39th annual American Astronomical Society, Division for Planetary Science meeting, Orlando, FL, 9 October 2007.
16. J. R. Spencer, K. L. Jessup, M. A. McGrath, G. E. Ballester, R. Yelle, *Science* **288**, 1208 (2000).
17. A. S. McEwen *et al.*, *Icarus* **135**, 181 (1998).
18. R. G. Strom, N. M. Schneider, in *Satellites of Jupiter*, D. Morrison, Ed. (Univ. of Arizona Press, Tucson, AZ, 1982), pp. 598–633.
19. J. Zhang *et al.*, *Icarus* **172**, 479 (2004).
20. J. A. Stansberry, J. R. Spencer, R. R. Howell, D. Vakili, *Geophys. Res. Lett.* **24**, 2455 (1997).
21. A. G. Davies *et al.*, *J. Geophys. Res.* **106**, 33079 (2001).
22. A. S. McEwen *et al.*, *Science* **281**, 87 (1998).
23. We thank the entire NH mission team, particularly D. Rose and E. Birath, and our colleagues on the NH science team. NH and the ancillary investigations described here are funded by NASA, whose financial support we gratefully acknowledge.

Supporting Online Material

www.sciencemag.org/cgi/content/full/318/5848/240/DC1

Fig. S1

Table S1

Movie S1

10 July 2007; accepted 19 September 2007

10.1126/science.1147621

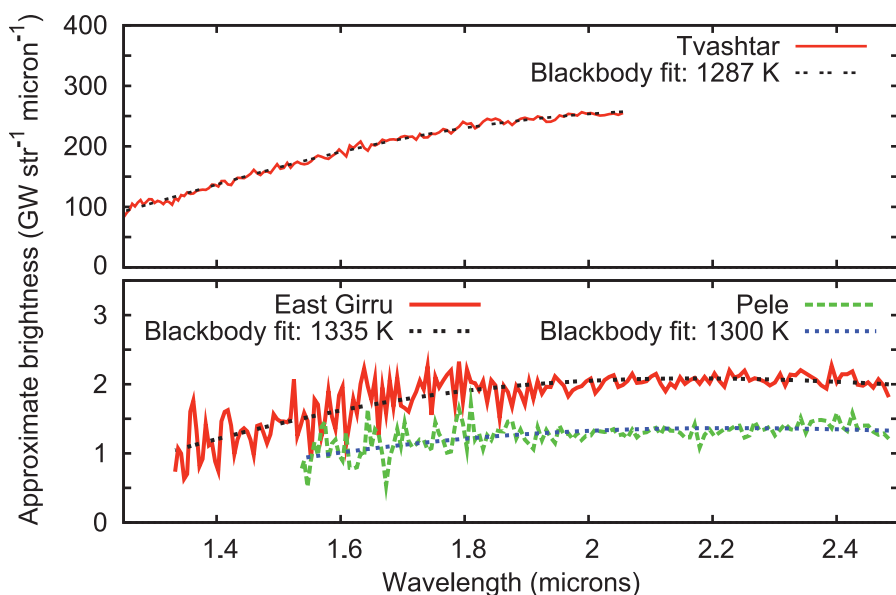


Fig. 4. LEISA spectra of volcanic thermal emission from Tvashtar, Pele, and East Girru, with best-fit blackbody curves superposed. Vertical axis units are $\text{GW steradian}^{-1} \mu\text{m}^{-1}$.